Mehran University Research Journal of Engineering and Technology

https://doi.org/10.22581/muet1982.0375

2025, 44(4) 133-142

Combatting emerging water contaminants: comparative photocatalytic degradation of pharmaceuticals using CeO_2/CdS nanorods under UV irradiation

Usman Niaz [a,b,c], Ayesha Jamil [d], M S Aziz [a, e*ab] and Retna Apsari [e,f]

[a] *Laser Centre, Ibnu Sina Institute for Scientific and Industrial Research, Universiti Teknologi Malaysia (UTM), 81310 Skudai, Johor, Malaysia*

[b] *Department of Physics, Faculty of Science, Universiti Teknologi Malaysia (UTM), 81310 Skudai, Johor, Malaysia*

[c] *Department of Physics, Science Division, University of Education, 54770 Lahore, Pakistan*

[d] *Building Research Station, Communication and Works Department, 54770 Lahore, Pakistan*

[e] *Department of Engineering, Faculty of Advanced Technology and Multidiscipline, Universitas Airlangga, Jl. Mulyorejo, Surabaya, 60115, Indonesia*

[f] *Department of Physics, Faculty of Science and Technology, Airlangga University, Surabaya 60115, Indonesia*

[*] Corresponding author: Prof. Ts. Muhammad Safwan Bin ABD Aziz, Email: safwanaziz@utm.my

Received: 01 June 2025, Revised: 27 August 2025, Accepted: 29 September 2025, Published: 01 October 2025

KEYWORDS

Efficient heterostructure

Photocatalysts

Diclofenac degradation

Bandgap engineering

Environmental remediation

Pharmaceutical pollutant

ABSTRACT

Pharmaceutical contamination in aquatic environments poses a critical global threat due to the persistence and toxicity of compounds such as Carbamazepine, Diclofenac, and Naproxen. In this study, fluorite-structured CeO_2/CdS composite nanorods were synthesized and evaluated for their photocatalytic efficiency in degrading these emerging contaminants under UV irradiation. The nanorods were thoroughly characterized using X-ray diffraction (XRD), field emission scanning electron microscopy (FESEM), Fourier-transform infrared (FTIR) spectroscopy, and UV-Vis spectroscopy. Structural analysis confirmed the successful integration of CdS into the CeO_2 matrix, and the average diameter (25 nm) was confirmed by FESEM. At the same time, optical characterization revealed a narrowed bandgap of 2.23 eV, enhancing UV light absorption. Photocatalytic experiments demonstrated significant degradation efficiencies, achieving 62.4% for Carbamazepine, 78.0% for Diclofenac, and 95.3% for Naproxen within 180 minutes of UV exposure with degradation rate constants of 0.0054 Min^{-1}, 0.008 Min^{-1}, and 0.015 Min^{-1}, respectively. The high degradation performance is attributed to the synergistic interaction between CeO_2 and CdS, which facilitates enhanced charge separation and photocatalytic reactivity. These findings highlight the potential of CeO_2/CdS nanorods as an effective and sustainable photocatalyst for the removal of pharmaceutical pollutants from water systems.

1. Introduction

The persistent contamination of aquatic ecosystems by pharmaceutical compounds has become an escalating global concern, driven by the extensive and often unregulated use of pharmaceuticals in human and veterinary medicine [1], [2]. Among these, Carbamazepine [3], Diclofenac [4], and Naproxen [5] are frequently detected in surface waters, wastewater effluents, and even drinking water due to their chemical stability, high consumption rates, and incomplete removal in conventional treatment processes [6]. These

© Mehran University of Engineering and Technology 2025

compounds are classified as emerging contaminants and are associated with endocrine disruption, chronic toxicity, and the promotion of antimicrobial resistance, posing serious risks to both environmental and public health [7]. The limitations of traditional wastewater treatment technologies have stimulated interest in advanced oxidation processes (AOPs), particularly semiconductor-based photocatalysis, as a promising strategy for the degradation of persistent organic pollutants [8]. Photocatalysis offers several advantages, including environmental compatibility,[9] low energy consumption [10], and the potential for complete mineralization of contaminants into non-toxic end products [11].

Among various photocatalysts, cerium oxide [12] (CeO_2) has garnered significant attention due to its unique fluorite-type crystal structure, oxygen storage capacity, and excellent redox cycling between Ce^{3+} and Ce^{4+} states [13]. However, its practical application is hindered by a wide bandgap and rapid recombination of photogenerated charge carriers [14], which limit its photocatalytic efficiency under UV light [15]. To overcome these challenges, coupling CeO_2 with a narrow-bandgap semiconductor such as cadmium sulfide (CdS) has emerged as an effective strategy [16], [17], [18]. CdS not only enhances visible-light absorption but also promotes efficient electron-hole separation through heterojunction formation [19], thereby improving overall photocatalytic activity. In this study, a combination of cerium dioxide (CeO_2) and cadmium sulfide (CdS) nanorods was synthesized and extensively studied to enhance the degradation of pharmaceutical pollutants. To synthesize the metal or semiconductor nanostructures, there are multiple methods like hydrothermal [20], microbes [21], laser matter interaction [22], Ion beam acceleration [23], and plant extracts[24]. Amongst all these methods, hydrothermal method has shown better performance in nanorods formation at bulk [25], hence this method is chosen for this study. Unlike before, this work checks the sequential degradation of three environmentally persistent pharmaceuticals, carbamazepine, diclofenac and naproxen, all exposed to UV light. Tests with XRD, FESEM, FTIR and UV-Vis spectroscopy confirmed the structures, shapes and optical qualities of the synthesized nanorods. In this study, the connection between material properties and photocatalytic performance gives an important direction for designing efficient composite nanomaterials for treating water. It is shown that CeO_2/CdS nanorods have high rates of degradation and can be used as a reliable and cost-effective way to remove pharmaceutical products in environmental water.

2. Materials and Methods

2.1 Experimental Materials

All the chemicals used, including Sodium Hydroxide (NaOH), Cerium Nitrate Hexahydrate ($Ce(NO_3)_3 \cdot 6H_2O$), Cadmium Nitrate Tetrahydrate ($Cd(NO_3)_2 \cdot 4H_2O$), Ethylenediamine ($NH_2CH_2CH_2NH_2$), Thiourea (NH_2CSNH_2) and deionised water, were supplied by Sigma-Aldrich and measured at least 99.9% pure. XRD analysis was carried out to check the crystalline structure and type of phases in the nanocomposites. A Field Emission Scanning Electron Microscope (FESEM) was used to examine the surface appearance and nanostructure of the sample. Using Energy Dispersive X-ray Spectroscopy (EDX), we proved that cerium and cadmium were found in the form of composites. The position and amounts of elements inside the samples were identified by Elemental Mapping. A Fourier Transform Infrared Spectroscopy (FTIR) analysis was done to determine the functional groups and bond patterns in the materials, and a UV-visible spectroscopy (UV-Vis) test was used to study their optical and band gap characteristics. All characterisation techniques were performed at the University-Industry Research Laboratory Services, UTM.

2.2 Experimental Methods

The experimental procedure is divided into two main sections. In the first section, CeO_2/CdS nanorods were synthesized via a solvothermal approach. In the second section, the synthesized nanorods were employed as photocatalysts to evaluate the degradation performance against three pharmaceutical pollutants: carbamazepine, diclofenac, and naproxen. Detailed methodologies for each phase are provided in the following subsections. Whereas, while dealing with the statistical data calculations including length measurements etc., the average of three independent trials was taken as the result.

2.2.1 Synthesis of CeO_2/CdS nanocomposites

The solvothermal technique prepared the CeO_2/CdS composite nanorods. 30 mg of the pre-prepared CeO_2

© Mehran University of Engineering and Technology 2025

nanorod powder, as synthesized in our previous study [25] was combined with 40 mL of ethylenediamine after being sonicated for 30 minutes. The solution was then rapidly agitated for 60 minutes after adding 0.398 g of thiourea and 0.537 g of cadmium nitrate tetrahydrate. After that, this solution was transferred to a 50 mL autoclave and maintained at 364 K for 24 hours. Following the solvothermal treatment, the precipitates known as "CeO_2/CdS composite nanorods" were cleaned and retrieved by centrifugation. After that, they were placed in a 335 K drying oven for the entire night. The schematic to illustrate the synthesis process of CeO2/CdS NRs is given in Fig. 1.

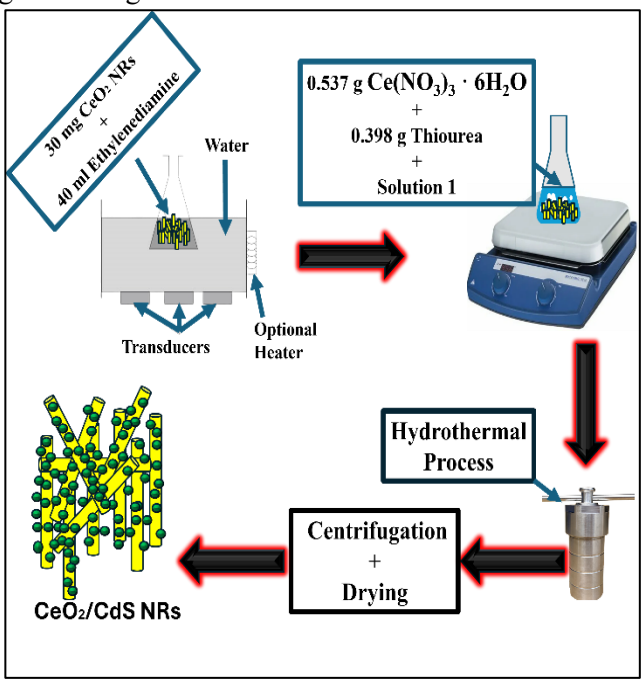

Fig. 1. Schematic illustration of CeO_2/CdS NRs synthesis process

2.2.2 Photocatalytic Activity Observation

To evaluate the photocatalytic degradation performance of the CeO_2/CdS composite nanorods, aqueous solutions of three pharmaceutical contaminants, Carbamazepine, Diclofenac, and Naproxen, were prepared by dissolving 30 mg of each compound in 1 L of deionized water. For each degradation test, 20 mg of the photocatalyst was added to 80 mL of the respective pollutant solution. The suspensions were ultrasonicated for 30 minutes and kept under dark conditions for an additional 90 minutes to ensure adsorption–desorption equilibrium between the catalyst surface and the pollutant molecules. Photocatalytic experiments were carried out in a 100 mL quartz reactor, the schematic is shown in Fig. 2. A 300 W Xenon lamp equipped with a UV filter was positioned 10 cm above the liquid surface to serve as the UV light source. Upon irradiation, 2 mL aliquots were withdrawn at regular intervals and immediately analyzed using UV–Vis spectroscopy to monitor the concentration change of each pharmaceutical over time. All experiments were conducted under identical conditions to ensure comparability of degradation efficiency across the three contaminants.

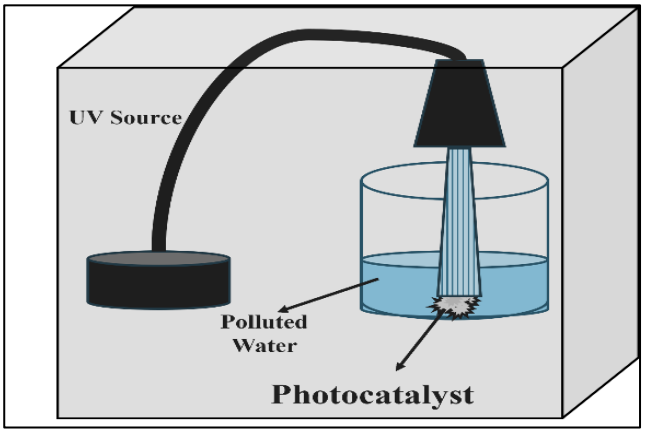

Fig. 2. Schematic illustration of photocatalysis setup

3. Results and Discussion

3.1 Structural Examination

The X-ray diffraction (XRD) patterns of the synthesized CeO_2/CdS composite nanorods, presented in Fig. 3, display distinct diffraction peaks corresponding to both cerium oxide and cadmium sulfide phases, confirming the successful formation of the composite material. The characteristic CeO_2 peaks observed at 28.54°, 33.07°, 47.55°, 56.22°, 59.05°, 69.26°, 76.75°, and 79.03° can be indexed to the (111), (200), (220), (311), (322), (400), (331), and (420) crystallographic planes, respectively, consistent with the fluorite-type face-centred cubic (FCC) structure of CeO_2 as referenced in PCPDF No. 81-0792 [12], [26]. Similarly, diffraction peaks attributable to CdS appear at 24.9° (100), 26.6° (002), 28.4° (101), 36.7° (102), 43.7° (110), 47.8° (103), 51.9° (112), and 66.8° (203), matching well with JCPDS No. 41-1049 [27], [28]. The coexistence of these peaks within the composite's diffraction pattern, along with minor peak shifts and broadening, suggests strong interfacial interactions and tight integration between the CeO_2 and CdS phases. This structural synergy not only validates the successful synthesis of the CeO_2/CdS composite nanorods but also supports the hypothesis of enhanced photocatalytic properties arising from their intimate heterojunction formation.

3.2 Morphological Examination

The morphological characteristics of the CeO_2/CdS composite nanorods were investigated using field emission scanning electron microscopy (FESEM). As

© Mehran University of Engineering and Technology 2025

illustrated in Figure 4(a), the composite exhibits a uniform nanorod morphology with well-defined, elongated structures. Quantitative analysis of the nanorod dimensions, presented in the histograms of Figures 4(b) and 4(c), reveals an average diameter of approximately 25 nm and an average length of about 229 nm. These dimensions correspond to high aspect ratio nanorods, which are beneficial for enhancing the specific surface area and facilitating improved photocatalytic performance by providing more active sites for pollutant degradation.

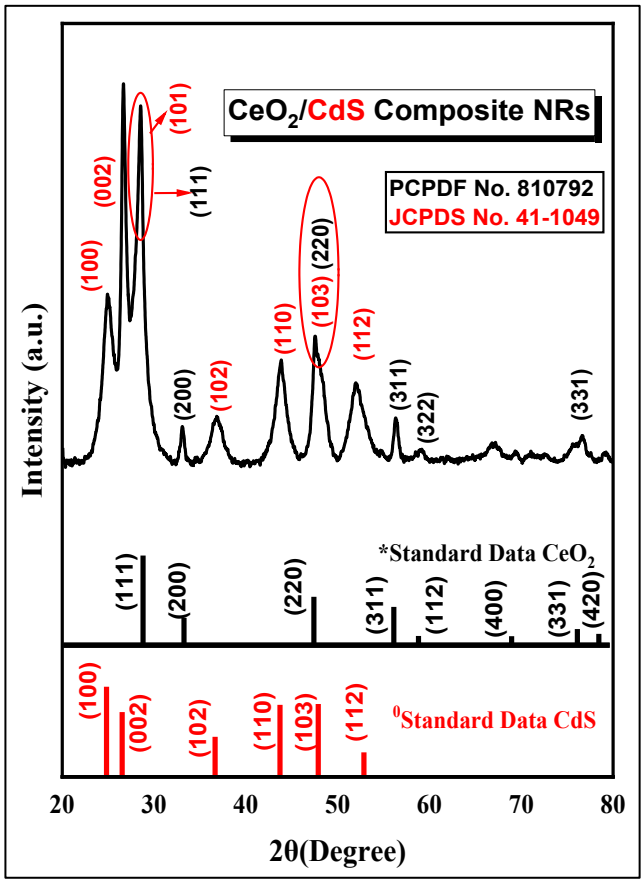

Fig. 3. XRD patterns of CeO_2/CdS composite nanorods showing characteristic peaks of fluorite-type FCC CeO_2 and overlapping CdS diffraction peaks, confirming successful composite formation.

3.3 Elemental Mapping and Compositional Analysis

Figure 5 presents the elemental mapping and energy-dispersive X-ray (EDX) analysis of the CeO_2/CdS composite nanorods. The FESEM elemental maps (Figure 5(a)) reveal a uniform and homogeneous distribution of cerium (Ce), oxygen (O), cadmium (Cd), and sulfur (S) throughout the nanorods, indicating the successful and intimate incorporation of CdS within the CeO_2 matrix. This consistent elemental dispersion, highlighted by the composite overlay map, is critical for facilitating efficient charge separation, a key factor enhancing photocatalytic performance. The EDX spectrum shown in Figure 5(b) confirms the presence of Ce, O, Cd, and S elements in proportions consistent with the intended composite composition. Notably, the absence of significant impurities underscores the purity and effectiveness of the synthesis protocol. Collectively, these findings validate the successful fabrication of well-defined CeO_2/CdS composite nanorods with uniform elemental distribution, supporting their potential for efficient photocatalytic degradation of pharmaceutical pollutants.

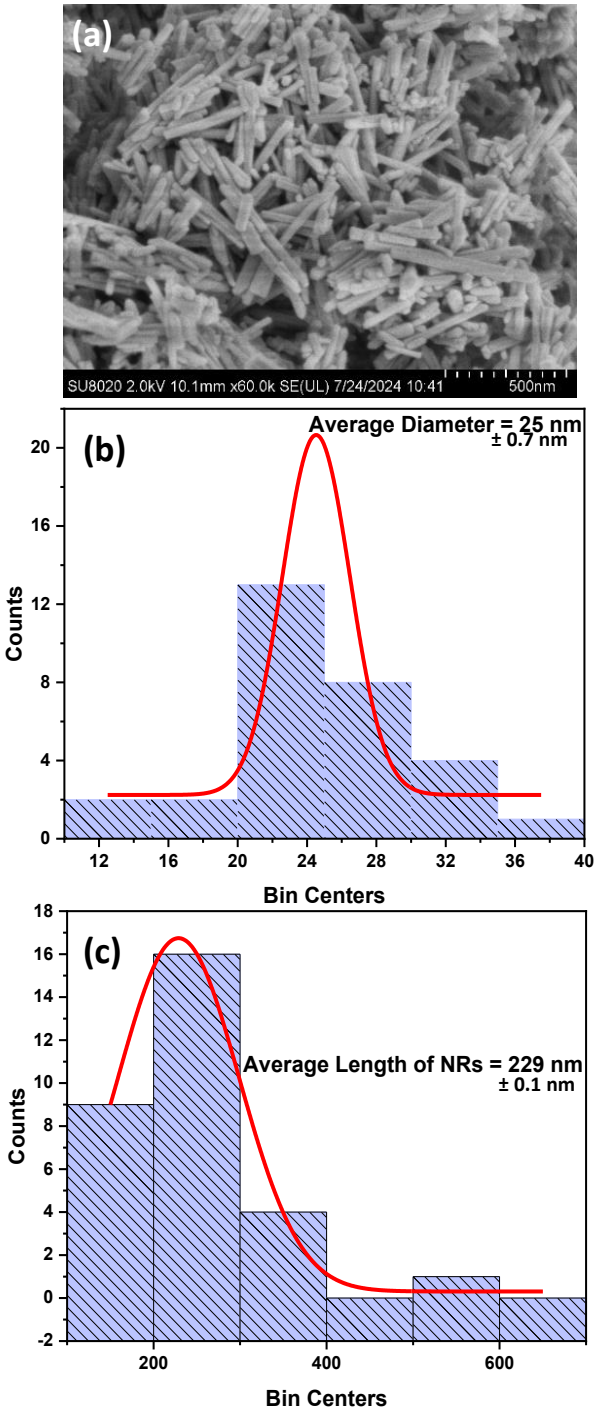

Fig. 4. (a) FESEM Image of CeO_2/CdS Composite Nanorods, Demonstrating Uniform Morphology; **(b)** Diameter Distribution Histogram with; **(c)** Length Distribution Histogram

3.4 FTIR Spectroscopy Analysis

The functional groups and bonding characteristics of the CeO_2/CdS composite nanorods were investigated using Fourier-transform infrared (FTIR) spectroscopy, as depicted in Figure 6. Four prominent absorption bands were identified at approximately 3300 cm^{-1},

© Mehran University of Engineering and Technology 2025

1670 cm^{-1}, 1120 cm^{-1}, and 1000 cm^{-1}, each corresponding to specific vibrational modes. The broad peak centered around 3300 cm^{-1} is attributed to O–H stretching vibrations [29], arising from surface-adsorbed hydroxyl groups or residual water molecules. These hydroxyl groups play a vital role in photocatalysis by acting as active sites for hydroxyl radical generation, which are key agents in degrading organic pollutants. The band near 1670 cm^{-1} corresponds to H–O–H bending vibrations, confirming the presence of adsorbed water on the catalyst surface. The peak observed at 1120 cm^{-1} is assigned to C–O stretching vibrations, indicating carbonate species likely formed due to atmospheric CO_2 adsorption during synthesis. These surface carbonate groups can influence the surface chemistry and, consequently, the catalytic activity. Importantly, the distinct peak around 1000 cm^{-1} arises from overlapping Ce–O and Cd–S vibrational modes [30], affirming the successful incorporation of both CeO_2 and CdS phases within the composite. The Ce–O bond reflects the characteristic fluorite structure of CeO_2, while the Cd–S bond signifies the presence of CdS nanoparticles. Hence, the FTIR analysis confirms the coexistence of essential functional groups and bonding interactions critical to the composite's photocatalytic efficiency. The combination of surface hydroxyl and carbonate groups, along with robust structural linkages, enhances the composite's ability to interact with light and organic contaminants, thereby promoting effective photocatalytic degradation.

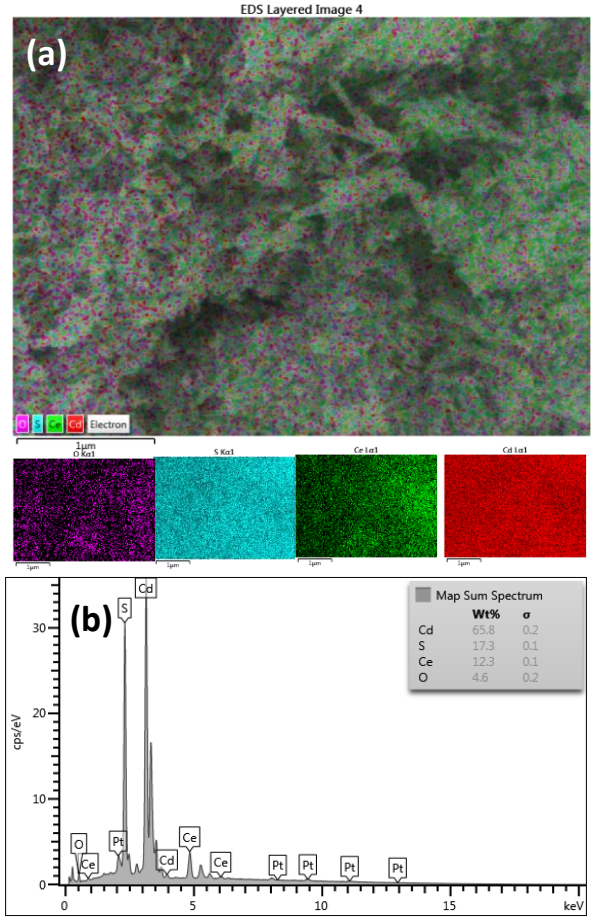

Fig. 5. (a) FESEM elemental mapping of CeO_2/CdS composite nanorods illustrating overlay map showing uniform elemental distribution of Ce, O, Cd, and S **(b)** Corresponding EDX spectrum confirming the presence of Ce, O, Cd, and S in the composite.

3.5 Optical Characteristics

To study the optical properties of CeO_2/CdS composite nanorods, UV-Vis spectroscopy was used and the absorbance spectrum along with the Tauc plot [31] are shown in Figure 7. Absorption in the visible light region is strong in this composite, which explains its potential for using visible light in photocatalytic processes. Since pure CeO_2 blocks only UV radiation due to its small window size, the composite shifts absorbance to the red parts of the visible spectrum. CdS plays a vital role because it adds its light harvesting power to that of CeO_2. Figure 7 shows an inset of a Tauc plot (assuming direct allowed transition for both CeO_2 and CdS), made from absorbance measurements, to measure the bandgap energy. By extending the effective straight section of $(\alpha h\nu)^2$ versus hv, the calculated bandgap for the composite comes to around 2.23 eV. CdS plays a key part in making CeO_2 work well with light, since little CeO_2 alone does not have this function.

Fig. 6. FTIR spectrum of CeO_2/CdS composite nanorods highlighting key functional groups and bonding vibrations.

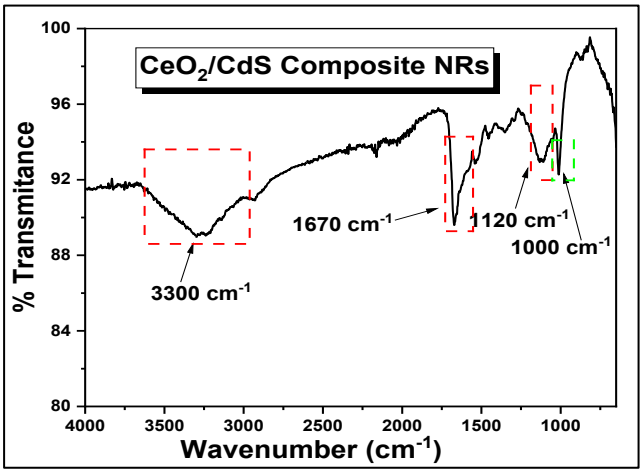

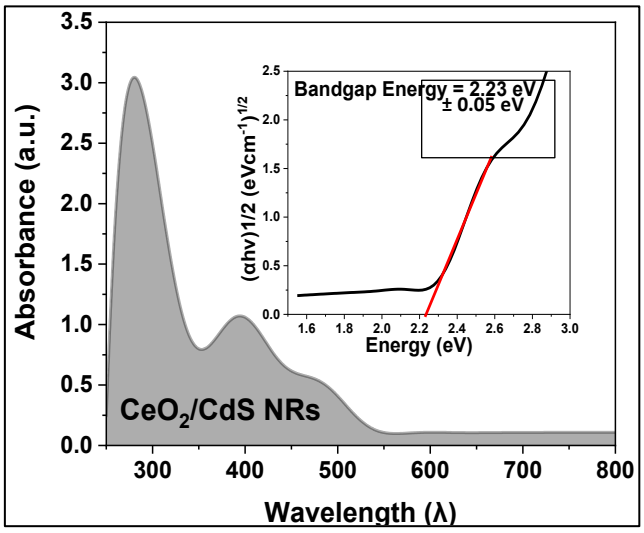

Fig. 7. UV-Vis absorbance spectrum of CeO_2/CdS composite nanorods exhibiting strong visible light absorption. Inset: Tauc plot used to estimate the bandgap energy.

© Mehran University of Engineering and Technology 2025

These optical features highlight the CeO_2/CdS composite nanorods as promising photocatalysts under visible light irradiation. The enhanced light absorption and reduced bandgap facilitate improved generation and separation of electron-hole pairs, thereby boosting photocatalytic degradation efficiency.

3.6 Photocatalytic Degradation of Carbamazepine, Diclofenac, and Naproxen under UV Irradiation Using CeO_2/CdS Composite Nanorods

The photocatalytic degradation performance of CeO_2/CdS composite nanorods was evaluated against three common pharmaceutical contaminants: Naproxen, Carbamazepine, and Diclofenac under UV light irradiation. UV-Vis spectroscopy was employed to monitor pollutant degradation, with results summarized in Figure 9. Before going towards the photocatalytic activity let's discuss the pathway of the photocatalytic activity process. Figure 8 illustrates the schematic of the mechanistic pathway of the degradation of carbamazepine, a similar pathway for the other pharmaceutical active compounds can also be observed. Figure 8 illustrates that the mechanism starts when light interacts with the photocatalyst, resulting in the formation of reactive oxygen species (ROS). These ROS interacts with the pollutants, resulting the breakdown of the pharmaceutical pollutants. The influence of solution's pH on the photocatalytic degradation, is well documented, with pH affecting the surface charge of the photocatalyst, the ionization state of pollutants, and the generation efficiency of reactive oxygen species (ROS) [32], [33]. In this work, the pH of the reaction mixture was kept unaltered to focus on the intrinsic activity of the prepared photocatalyst. A detailed investigation of pH-dependent performance is planned for future studies.

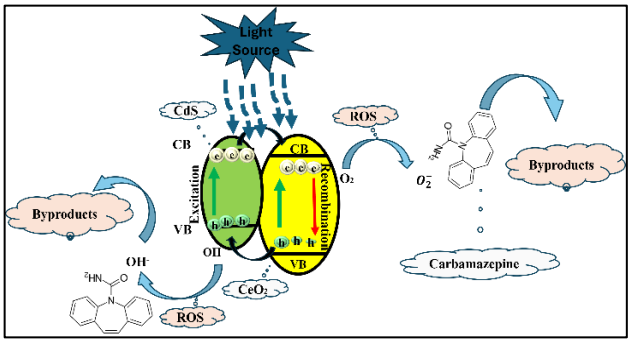

Fig. 8. Mechanistic pathway of the degradation of carbamazepine utilizing CeO_2/CdS NRs

Further, as shown in Figure 9(a), Naproxen degradation exhibited a significant increase over 180 minutes, reaching an impressive 95.32%. This high degradation efficiency underscores the composite's strong photocatalytic activity against Naproxen under UV light. Similarly, Figure 9(b) demonstrates the effective breakdown of Carbamazepine, with degradation rates rising steadily from 13.4% at early exposure to 62.4% after 180 minutes. Diclofenac degradation, depicted in Figure 9(c), also followed a comparable trend, improving from 23% initially to 78% at the end of the irradiation period. Whereas Figure 9(d) represents the comparison of efficiencies across all the pollutants. The progressive increase in degradation efficiency for all three pharmaceuticals highlights the CeO_2/CdS composite's robust photocatalytic capabilities under UV light. Moreover, blank and dark experiments for all three pollutants were also done for the sake of better comparison, notably, there was no major degradation found in any of the samples. These dark and blank experiments proved that the degradation observed is purely the effect of the presence of photocatalyst and the interaction of light with the catalyst.

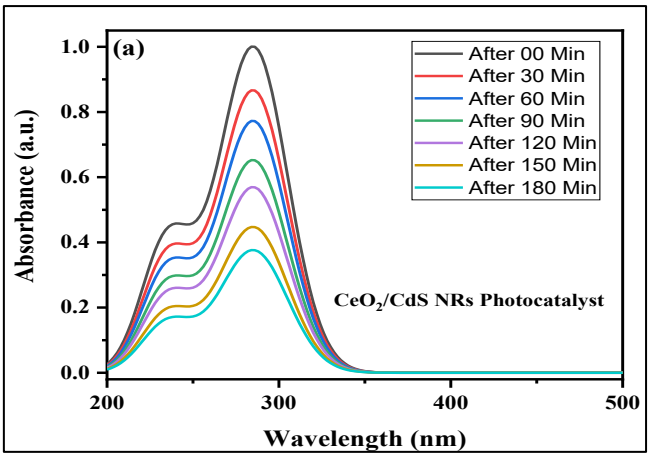

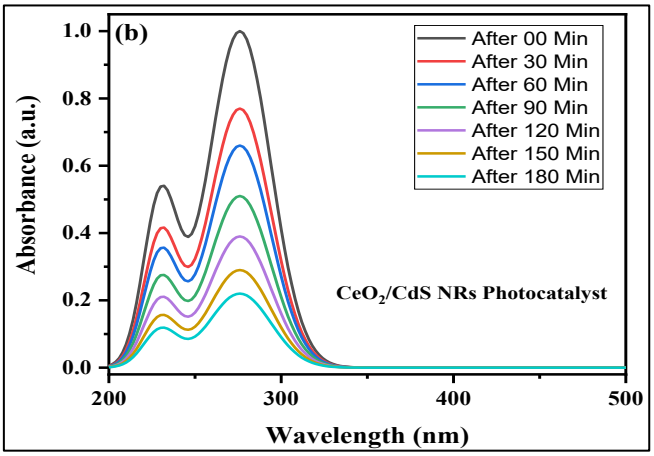

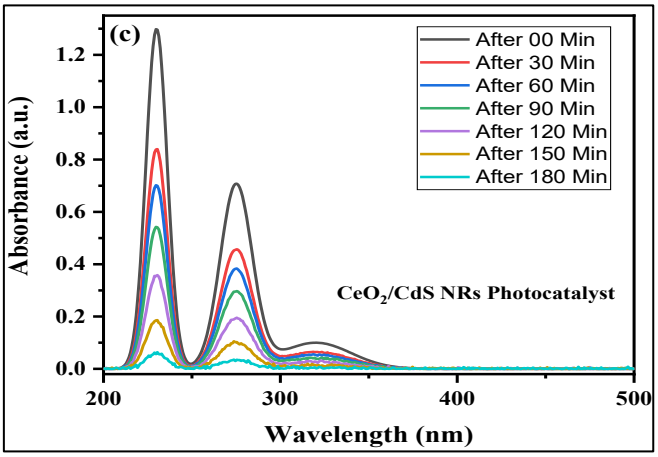

© Mehran University of Engineering and Technology 2025

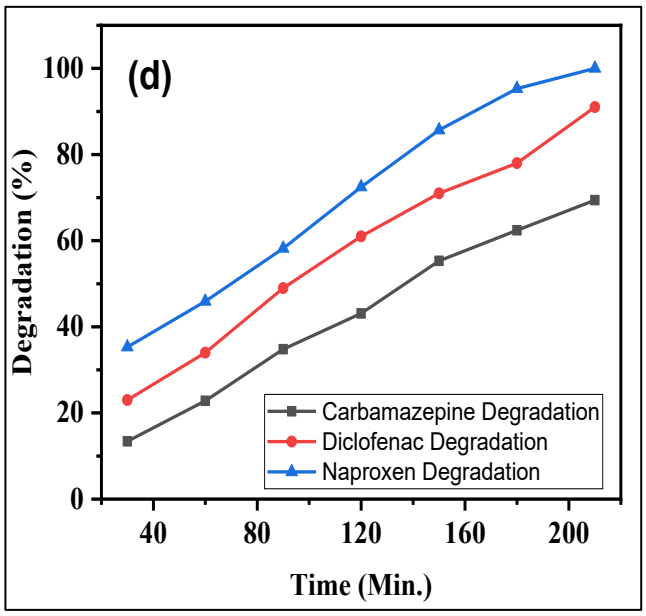

Fig. 9. Photocatalytic degradation performance of CeO_2/CdS composite nanorods: **(a)** UV-Vis spectra showing degradation of carbamazepine (**b)** UV-Vis spectra showing degradation of diclofenac **(c)** UV-Vis spectra showing degradation of naproxen **(d)** Comparative Degradation Efficiency of Naproxen, Carbamazepine, and Diclofenac under UV Irradiation.

This performance is attributed to the synergistic effect between CeO_2 and CdS, which facilitates efficient electron-hole pair generation and separation, thereby promoting oxidative degradation of the pollutants. The composite's tailored bandgap (~2.23 eV) further supports effective light absorption and catalytic activity. Overall, these results demonstrate that CeO_2/CdS composite nanorods offer a potent and sustainable solution for the removal of hazardous pharmaceutical contaminants from water using UV-driven photocatalysis.

Figure 10 and Table 1 list the degradation efficiencies, degradation rate constants and correlation coefficients for each pharmaceutical contaminant treated with CeO_2/CdS composite nanorods (NRs). The illustration shows the effectiveness of the photocatalyst when removing different pollutants. Of all the tested pharmaceuticals, naproxen had the highest rate of degradation (95.25%) and the highest rate constant considered (k = 0.015 min^{-1}). Because the R-square is high (0.90), it can be concluded that photocatalysis is happening fast and effectively, yet a slight variation at the end might be due to byproducts or a more complex process. 78% of diclofenac was degraded with a rate constant of 0.0083 min^{-1}, its degradation followed a steady and reliable pattern (R^2 = 0.99). Carbamazepine was found to degrade at only 62.4%, but it showed a high R^2 value (0.98), proving that its degradation was predictable even when slow. Because of their nanorod form, the CeO_2/CdS composites proved effective for all kinds of degradations, with naproxen being like the recipe providing the best results, thanks to its chemical structure or stronger interaction with the reactive oxygen species formed. These findings reinforce the potential of CeO_2/CdS composites for environmental remediation of pharmaceutical pollutants, with notable efficiency and kinetic reliability.

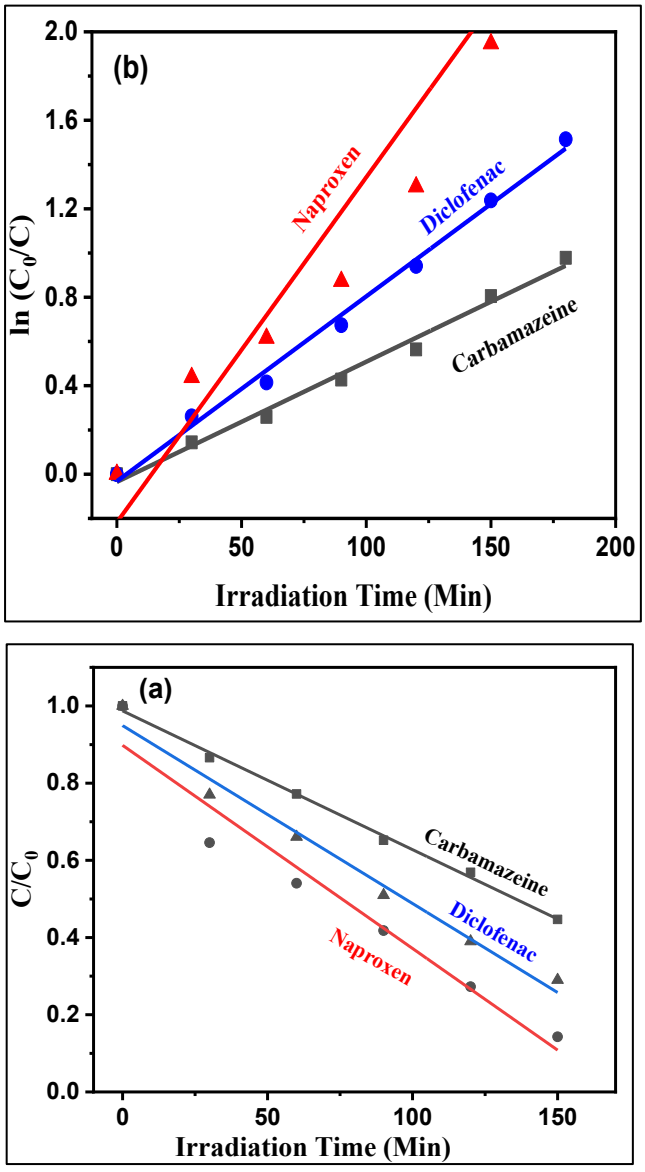

Fig. 10. (a) Photocatalytic activity **(b)** kinetics of pharmaceutical degradation in the presence of CeO_2/CdS NRs

Table 1

Summary of the characteristics of pharmaceutical degradation in the presence of CeO_2/CdS composite NRs

Catalyst	Degradation (%)	Degradation Rate Constant "k" (Min^{-1})	Correlation Coefficient R^2
Carbamazepine	62.4	0.0054	0.98
Diclofenac	78	0.0083	0.99
Naproxen	95.25	0.015	0.90

© Mehran University of Engineering and Technology 2025

4. Stability and reusability

The stability and reusability of the photocatalyst were also assessed following the same process as in our previous study on CeO_2 [25]. over the three consecutive photocatalytic degradation cycles of 210 minutes each, under identical conditions. After each cycle, the photocatalyst was recovered by centrifugation, washed with water and ethanol, dried at 60 °C, and reused under the same conditions. Diclofenac was chosen for the reusability test. There was only a slight decrease in degradation efficiency, even after the third cycle as shown in Fig. 11; the degradation efficiency reached 86.78% from 91.2% after 210 minutes of radiation exposure. This is indicating good structural stability and sustained activity. The marginal loss in performance may be attributed to minor surface fouling or active site blocking during repeated use. These findings suggest that the prepared photocatalyst is a promising candidate for practical wastewater treatment applications.

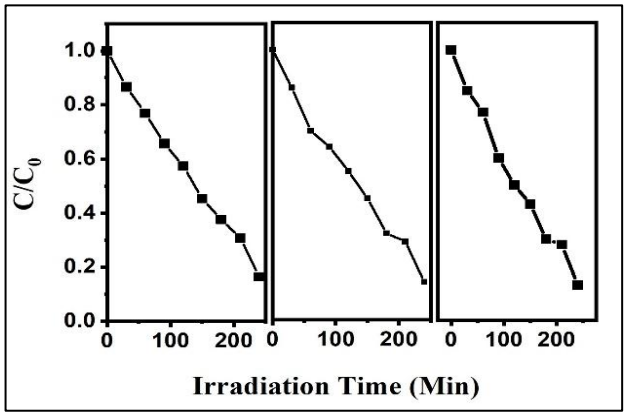

Fig. 11. Photocatalytic Degradation of diclofenac over three consecutive cycles to test the reusability

5. Conclusion

This study successfully synthesized and thoroughly characterized CeO_2/CdS composite nanorods with a fluorite-type structure, demonstrating their promising structural, morphological, optical, and photocatalytic properties. XRD analysis confirmed the formation of the CeO_2 fluorite-type FCC phase integrated with CdS, while FESEM and elemental mapping verified the uniform nanorod morphology and homogeneous elemental distribution. FTIR spectroscopy revealed key functional groups and bonding interactions that enhance photocatalytic activity. UV-Vis spectroscopy indicated a significant redshift in light absorption with a reduced bandgap energy of 2.23 eV, enabling efficient utilization of visible light. Importantly, the photocatalytic performance of the composite was evaluated through the degradation of multiple pharmaceutical contaminants, naproxen, carbamazepine, and diclofenac under UV irradiation. The composite exhibited remarkable degradation efficiencies of up to 95.32% for Naproxen, 78% for Diclofenac, and 62.4% for Carbamazepine after 180 minutes, highlighting its broad-spectrum efficacy and practical potential for water remediation. The enhanced photocatalytic activity is attributed to the synergistic interaction between CeO_2 and CdS, which promotes effective charge separation and extends light absorption into the visible region. These findings underscore the CeO_2/CdS composite nanorods as a highly effective, sustainable photocatalyst for the removal of hazardous pharmaceutical pollutants, contributing valuable insight toward addressing pressing environmental contamination challenges. In future studies, the comparison of different CeO_2/CdS composite NRs will be discussed in detail to observe the effect pH variation on photocatalytic degradation efficiency.

Acknowledgment

This work was supported by Universiti Teknologi Malaysia (UTM) under Matching Grant MG2 - 6.1 with cost center number Q.J130000.3009.04M29 and UTM Fundamental Research with cost center number Q.J130000.3809.22H43

6. References

[1] A. El Kaffas, J. M. Vo-Phamhi, J. F. Griffin, and K. Hoyt, “Critical Advances for Democratizing Ultrasound Diagnostics in Human and Veterinary Medicine,” *Annu Rev Biomed Eng*, vol. 26, no. 1, pp. 49–65, Jul. 2024, doi: 10.1146/annurev-bioeng-110222-095229.

[2] M. Rohan Khizer *et al.*, “Polymer and graphitic carbon nitride based nanohybrids for the photocatalytic degradation of pharmaceuticals in wastewater treatment – A review,” *Sep Purif Technol*, vol. 350, p. 127768, Dec. 2024, doi: 10.1016/j.seppur.2024.127768.

[3] Z. H. Mussa and F. F. Al-Qaim, “Impact of Anode Materials on Electrochemical Degradation of Carbamazepine: A Case Study of Producing the Main By-Product 10,11-Epoxycarbamazepine after Electrochemical Degradation of Carbamazepine,” *Indonesian Journal of Chemistry*, vol. 22, no. 4, p. 929, Jul. 2022, doi: 10.22146/ijc.71976.

[4] P. D, C. R. J, R. D. D, M. R M, and S. E, “Sustainable Solutions: ZnO Nanoparticles for Enhanced Photocatalytic Treatment of Paracetamol and Diclofenac,” *Water Air Soil*

© Mehran University of Engineering and Technology 2025

Pollut, vol. 236, no. 5, p. 309, May 2025, doi: 10.1007/s11270-025-07957-5.

[5] M.-W. Ha and S.-M. Paek, "Recent Advances in the Synthesis of Ibuprofen and Naproxen," *Molecules*, vol. 26, no. 16, p. 4792, Aug. 2021, doi: 10.3390/molecules26164792.

[6] P. Manyepa *et al.*, "Removal and risk assessment of emerging contaminants and heavy metals in a wastewater reuse process producing drinkable water for human consumption," *Chemosphere*, vol. 361, p. 142396, Aug. 2024, doi: 10.1016/j.chemosphere.2024.142396.

[7] E. P. Munzhelele, R. Mudzielwana, W. B. Ayinde, and W. M. Gitari, "Pharmaceutical Contaminants in Wastewater and Receiving Water Bodies of South Africa: A Review of Sources, Pathways, Occurrence, Effects, and Geographical Distribution," *Water (Basel)*, vol. 16, no. 6, p. 796, Mar. 2024, doi: 10.3390/w16060796.

[8] A. E. Gahrouei, S. Vakili, A. Zandifar, and S. Pourebrahimi, "From wastewater to clean water: Recent advances on the removal of metronidazole, ciprofloxacin, and sulfamethoxazole antibiotics from water through adsorption and advanced oxidation processes (AOPs)," *Environ Res*, vol. 252, p. 119029, Jul. 2024, doi: 10.1016/j.envres.2024.119029.

[9] A. Hayat *et al.*, "The photocatalytic H2O2 production: Design strategies, Photocatalyst advancements, environmental applications and future prospects," *Coord Chem Rev*, vol. 522, p. 216218, Jan. 2025, doi: 10.1016/j.ccr.2024.216218.

[10] Y. Ahmadi and K.-H. Kim, "Modification strategies for visible-light photocatalysts and their performance-enhancing effects on photocatalytic degradation of volatile organic compounds," *Renewable and Sustainable Energy Reviews*, vol. 189, p. 113948, Jan. 2024, doi: 10.1016/j.rser.2023.113948.

[11] N. N. Roslan *et al.*, "Recent Advances in Advanced Oxidation Processes for Degrading Pharmaceuticals in Wastewater—A Review," *Catalysts*, vol. 14, no. 3, p. 189, Mar. 2024, doi: 10.3390/catal14030189.

[12] U. Niaz *et al.*, "Laser-enhanced and UV-driven photocatalysis for the degradation of methylene blue using CeO2 nanostructures; A comparative study," *J Phys Conf Ser*, vol. 2974, no. 1, p. 012017, Mar. 2025, doi: 10.1088/1742-6596/2974/1/012017.

[13] Z. Guan, Y. Chen, W. Han, Y. Jiao, S. Liang, and G. Tian, "Engineering tandem double p-n heterostructured CeO2@CdS-Cu8S5 hollow spheres for remarkable photocatalytic CO2 reduction," *Appl Surf Sci*, vol. 616, p. 156433, Apr. 2023, doi: 10.1016/j.apsusc.2023.156433.

[14] X. Xu, C. Shao, J. Zhang, Z. Wang, and K. Dai, "Rational Design of S-Scheme CeO2/Bi2MoO6 Microsphere Heterojunction for Efficient Photocatalytic CO2 Reduction," *Acta Physico-Chimica Sinica*, vol. 40, no. 10, p. 2309031, Oct. 2024, doi: 10.3866/PKU.WHXB202309031.

[15] Y. Yan *et al.*, "Recent Advances of CeO2 - Based Composite Materials for Photocatalytic Applications," *ChemSusChem*, vol. 17, no. 14, Jul. 2024, doi: 10.1002/cssc.202301778.

[16] K. Yang *et al.*, "Recent advances in CdS-based photocatalysts for CO2 photocatalytic conversion," *Chemical Engineering Journal*, vol. 418, p. 129344, Aug. 2021, doi: 10.1016/j.cej.2021.129344.

[17] P. Zhang, Y. Liu, B. Tian, Y. Luo, and J. Zhang, "Synthesis of core-shell structured CdS@CeO2 and CdS@TiO2 composites and comparison of their photocatalytic activities for the selective oxidation of benzyl alcohol to benzaldehyde," *Catal Today*, vol. 281, pp. 181–188, Mar. 2017, doi: 10.1016/j.cattod.2016.05.042.

[18] F. C. Zenebe, A. M. Taddesse, M. Sivasubramanian, and N. B. G., "Highly efficient CdS/CeO2/Ag3PO4 nanocomposite as novel heterogenous catalyst for Knoevenagel condensation and acetylation reactions," *Heliyon*, vol. 10, no. 11, p. e31798, Jun. 2024, doi: 10.1016/j.heliyon.2024.e31798.

[19] M. Mahamud, A. M. Taddesse, Y. Bogale, and Z. Bezu, "Zeolite supported CdS/TiO2/CeO2 composite: Synthesis, characterization and photocatalytic activity for methylene blue dye degradation," *Mater Res Bull*, vol. 161, p. 112176, May 2023, doi: 10.1016/j.materresbull.2023.112176.

[20] A. N. Bugrov, V. K. Vorobiov, M. P. Sokolova, G. P. Kopitsa, S. A. Bolshakov, and M. A. Smirnov, "Hydrothermal synthesis of CeO2 nanostructures and their

© Mehran University of Engineering and Technology 2025

electrochemical properties," *Nanosystems: Physics, Chemistry, Mathematics*, vol. 11, no. 3, pp. 355–364, Jun. 2020, doi: 10.17586/2220-8054-2020-11-3-355-364.

[21] Md. A. Ali *et al.*, "Advancements in Plant and Microbe-Based Synthesis of Metallic Nanoparticles and Their Antimicrobial Activity against Plant Pathogens," *Nanomaterials*, vol. 10, no. 6, p. 1146, Jun. 2020, doi: 10.3390/nano10061146.

[22] U. Niaz, S. Hemat, A. Jamil, and M. S. Aziz, "Exploring the relationship between confinement geometry and the formation of high-quality silver nanoparticles by laser ablation in liquid media," *Indian Journal of Physics*, May 2024, doi: 10.1007/s12648-024-03251-y.

[23] Niaz U, Rafique MS, Jamil A, Ali B, and Tahir MB, "FABRICATION OF TUNGSTEN CARBIDE NANOPARTICLES BY ELECTROCHEMICAL ETCHING OF TUNGSTEN IONS IMPLANTED SUBSTRATE," *Science International*, vol. 27, no. 4, Jul. 2015.

[24] H. Chandra, P. Kumari, E. Bontempi, and S. Yadav, "Medicinal plants: Treasure trove for green synthesis of metallic nanoparticles and their biomedical applications," *Biocatal Agric Biotechnol*, vol. 24, p. 101518, Mar. 2020, doi: 10.1016/j.bcab.2020.101518.

[25] U. Niaz, A. A. Salim, A. Jamil, M. S. Salleh, R. Apsari, and M. S. Aziz, "Optimized Photocatalytic Degradation of Naproxen in Aquatic Environments Using Cerium Oxide Nanostructures: Morphological Effects and Laser-Enhanced Performance," *Mater Chem Phys*, p. 131337, Jul. 2025, doi: 10.1016/j.matchemphys.2025.131337.

[26] K. Liu *et al.*, "Synergistic Acceleration of CO2 Electroreduction Kinetics by Oxygen Vacancy and Heterogeneous Interface for Efficient HCOOH Production," *Adv Funct Mater*, Mar. 2025, doi: 10.1002/adfm.202424357.

[27] S. Wang *et al.*, "The Zn Vacancy-Mediated De-Accumulation Based Process for Hydrogen Production Performance Promotion of 1D Zn─Cd─S Nanorods," *Small*, vol. 20, no. 24, Jun. 2024, doi: 10.1002/smll.202306447.

[28] P. Dolma, N. Padha, A. Banotra, R. Niranjan, and Z. Hussain, "Effect of change in substrate temperature, layer thickness on the behaviour of n-CdS thin films and formation of their diodes and photovoltaic cell," *Thin Solid Films*, vol. 802, p. 140459, Aug. 2024, doi: 10.1016/j.tsf.2024.140459.

[29] J. Xia, J. Tian, T. Sun, J. Fan, and E. Liu, "Conductive Co1.5MoS3.2 promoted photocatalytic H2 production over g-C3N4.," *Surfaces and Interfaces*, vol. 47, p. 104218, Apr. 2024, doi: 10.1016/j.surfin.2024.104218.

[30] Z. Zhao *et al.*, "Cobalt enhanced (H/C-CdS)/CeO2 activity for visible light catalytic oxidation of formaldehyde at room temperature," *Appl Surf Sci*, vol. 657, p. 159672, Jun. 2024, doi: 10.1016/j.apsusc.2024.159672.

[31] P. R. Jubu *et al.*, "Considerations about the determination of optical bandgap from diffuse reflectance spectroscopy using the tauc plot," *Journal of Optics*, vol. 53, no. 5, pp. 5054–5064, Nov. 2024, doi: 10.1007/s12596-024-01741-0.

[32] V. Gadore, S. R. Mishra, and Md. Ahmaruzzaman, "One-pot synthesis of CdS/CeO2 heterojunction nanocomposite with tunable bandgap for the enhanced advanced oxidation process," *Sci Rep*, vol. 13, no. 1, p. 7708, May 2023, doi: 10.1038/s41598-023-34742-3.

[33] S. A. B. Gilani *et al.*, "pH dependent synthesis of ceria nanoparticles for efficient sunlight-driven photocatalysis of methyl orange containing wastewater," *Opt Mater (Amst)*, vol. 148, p. 114871, Feb. 2024, doi: 10.1016/j.optmat.2024.114871.

© Mehran University of Engineering and Technology 2025